Control of exit flow and thermal conditions using two-layered thin films supported by flexible complex seals

A.-R.A. Khaled [a], K. Vafai [b,*]

[a] *Department of Mechanical Engineering, The Ohio State University, Columbus, OH 43210, USA*
[b] *Department of Mechanical Engineering, University of California at Riverside, Riverside, CA 92521, USA*

Abstract

This work considers flow and heat transfer inside an oscillatory disturbed two-layered thin film channel supported by flexible complex seals in the presence of suspended ultrafine particles. The governing continuity, momentum and energy equations for both layers are non-dimensionalized and categorized for small Reynolds numbers and negligible axial conduction. The deformation of the supporting seals is linearly related to both the pressure difference across the two layers and the upper plate's temperature based on the theory of the linear elasticity and the principle of the volumetric thermal expansion applied to the closed voids within the seals. It is found that the flow rate and heat transfer in the main thin film channel can be increased by an increase in the softness of the seals, the thermal squeezing parameter, the thermal dispersion effect and the total thickness of two-layered thin film. However, they decrease as the dimensionless thermal expansion coefficient of the seals and the squeezing number of the main layer increase. Both the increase in thermal dispersion and in the thermal squeezing parameter for the secondary layer are found to increase the stability of the intermediate plate. Furthermore, the two-layered thin film channel is found to be more stable when the secondary flow is free of pulsations or it has relatively a large pulsating frequency. Finally, the proposed two-layered thin film supported by flexible complex seals unlike other controlling systems does not require additional mechanical control or external cooling devices.
© 2003 Elsevier Ltd. All rights reserved.

Keywords: Two-layered thin films; Squeezing; Thermal dispersion; Heat transfer; Seals; Thermal expansion

1. Introduction

Thin films are widely used in the industry. For example they are used for cooling of electronic components [1,2]. They are widely encountered in film lubrication applications [3]. In biological applications, Lavrik et al. [4] and Fritz et al. [5] tested a novel biosensor experimentally which was placed inside a thin film fluidic cell. Although thin films are characterized by having laminar flows with relatively low Reynolds numbers leading to stable hydrodynamic performance, their thickness is small enough such that small disturbances at one of the boundaries may cause significant squeezing effect at this boundary.

Several authors analyzed flow between squeezed thin films like Langlois [6] who considered flow inside isothermal oscillatory squeezed films with fluid density varying with the pressure. Khaled and Vafai [7,8] discussed flow and heat transfer inside incompressible thin films having a prescribed oscillatory squeezing at one of their boundaries. Khaled and Vafai [9] considered also the squeezing effect caused by the internal pulsative pressure due to the elastic behavior of the supporting seal. They demonstrated that cooling is enhanced either by having soft seals or increasing the pressure levels inside the thin film.

Recently, Khaled and Vafai [10] discussed the situation where the squeezing effect at the free plate is initiated by thermal effects. They pointed out that this action

* Corresponding author. Tel.: +1-909-787-2135; fax: +1-909-787-2899.
E-mail address: vafai@engr.ucr.edu (K. Vafai).

Nomenclature

B	thin film length
C_F	correction factor for the volumetric thermal expansion coefficient
C_p	specific heat of the fluid
D	width of the thin film
E^*	softness index of seals supporting the intermediate plate
G	width of stagnant fluid cell
H_t	dimensionless total thickness of the two-layered thin film
F_T	dimensionless coefficient of the thermal expansion for the complex seal
H, h, h_0	dimensionless, dimensional and reference thin film thickness
h_c	convective heat transfer coefficient
K^*	effective stiffness of the sealing
k	thermal conductivity of the fluid
k_0	reference thermal conductivity of the fluid
Nu	lower plate's Nusselt number
P_S	thermal squeezing parameter
p	fluid pressure
q_0	reference heat flux at the lower plate for UHF
T, T_0	temperature in fluid and the inlet temperature
t	time
V_0	reference axial velocity
U, U_m	dimensionless axial and average axial velocities
u	dimensional axial velocity
V, v	dimensionless and dimensional normal velocities
X, x	dimensionless and dimensional axial coordinates
Y, y	dimensionless and dimensional normal coordinates

Greek symbols

α	thermal diffusivity of the fluid
β_q	dimensionless amplitude of the thermal load
β_p	dimensionless amplitude of the pressure
β_T	coefficient of volumetric thermal expansion
ε	perturbation parameter
φ_p	phase shift angle
γ	dimensionless frequency of the thermal load
γ_p	dimensionless frequency of the internal pressure
μ	dynamic viscosity of the fluid
θ, θ_m	dimensionless temperature and dimensionless mean bulk temperature
ρ	density of the fluid
τ, τ^*	dimensionless time
σ	squeezing number
ω	reciprocal of a reference time (reference squeezing frequency)
η	variable transformation for the dimensionless Y-coordinate
λ	dimensionless dispersion parameter
Π	dimensionless pressure
Π_n	dimensionless inlet pressure
Λ	reference lateral to normal velocity ratio

Subscripts

i	ith layer
l	lower plate
p	due to pressure
t	due to thermal expansion
u	upper plate

can be achieved by utilizing a new sealing assembly that is composed of soft seals with voids of stagnant fluids having relatively large volumetric thermal expansion coefficient. They named this sealing assembly as a flexible complex seal. This arrangement in a single layer thin film, can cause flooding of the coolant when the thermal load of the thin film is increased over its projected capacity. As a result, an enhancement in the cooling process is attained especially if ultrafine suspensions are present in the coolant.

In this work, flexible complex seals in two-layered thin films are utilized in order to regulate the flow rate of the main layer such that excessive heating in the second layer results in a reduction in the main flow rate. This might find its applications in internal combustion industry where the fuel flow rate should be reduced as the engine gets overheated. Moreover, exit thermal conditions will be analyzed in two-layered thin films supported by flexible complex seals in order to investigate its feasibility in minimizing bimaterial effects of many biosensors. This is because many biosensors contain bimaterial components such as a microcantilever which is very sensitive to flow temperatures [5].

Oscillatory generic disturbances are imposed on the two-layered thin film channels supported by flexible complex seals in the presence of suspended ultrafine particles. These correspond to disturbances in the upper plate temperature and in the inlet pressure of the secondary layer. The governing continuity, momentum and energy equations for both layers are non-dimensionalized and categorized to meet certain physical conditions. The deformation of the supporting seals and accordingly the displacement of the intermediate plate are linearly related to both the pressure difference across the two

layers and the upper plate's temperature based on the theory of linear elasticity and the principle of the volumetric thermal expansion coefficient of the stagnant fluid filling the voids of the supporting flexible complex seals.

2. Problem formulation and analysis

Fig. 1 shows a two-layered thin film supported by flexible complex seals. The lower layer contains the main flow passage where its lower plate is fixed and its upper plate is insulated and free to move in the vertical direction. The main flow can be the fuel flow or fuel-air mixture prior to combustion or flow of a biofluid in a fluidic cell. The upper layer of the thin film contains a secondary flow parallel or counter to the main flow direction. This flow can have similar properties as the main flow. This suits fluidic cell applications since inlet pressure pulsations will be equal across the intermediate plate thus disturbances at the intermediate plate will be
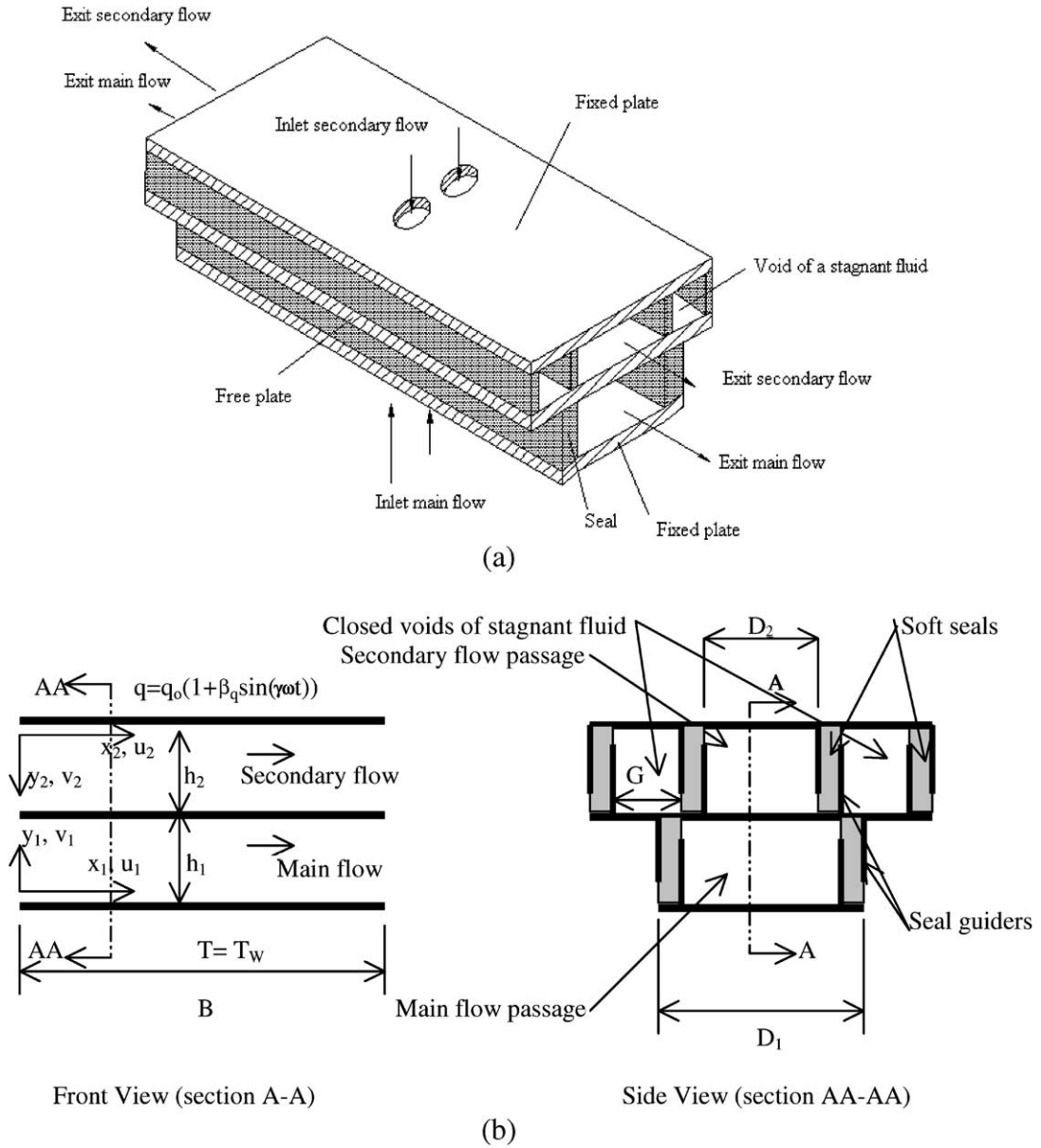
Fig. 1. Schematic diagram for a two-layered thin film supported by flexible complex seals: (a) three dimensional view and, (b) front and side views.

eliminated. The secondary flow, however, can have different properties than the main flow. Such would the case when the secondary flow is initiated from external processes such as flow of combustion residuals or the engine coolant flow.

The upper layer of the two-layered thin film shown in Fig. 1 is composed of the secondary flow passage and a sealing assembly where its upper plate is fixed and subjected to a prescribed heat flux. This heat flux can be independent of the main flow or can be the result of external processes utilizing the main flow as in combustion processes. The latter can be used for controlling the main flow conditions while the former may model the increase in the ambient temperature in a fluidic cell application. This can prevent an increase in the average fluid temperature in an ordinary fluidic cell thus avoiding a malfunctioning of the biosensor.

The sealing assembly of the upper layer contains closed voids filled with a stagnant fluid having a relatively large volumetric thermal expansion coefficient. This sealing assembly contains also soft seals in order to allow the intermediate plate to move in the normal direction (Fig. 1). Any excessive heating at the upper plate results in an increase in the upper plate's temperature thus the stagnant fluid becomes warmer and expands. This expansion along with the increase in inlet pressure in the upper layer, if present, cause the intermediate plate to move downward. Thus, a compression in the film thickness of the lower layer is attained resulting in reduction in mass flow rate within the main flow compartment. This arrangement, as mentioned before is needed to control combustion rates since part of the excessive heating and increased pressure due to deteriorated combustion conditions can be utilized to prescribe the heat flux at the upper plate. Thus, the flow rate of the fuel in the main layer can be reduced and combustion is controlled.

In fluidic cells, excessive heating at the upper plate causes compression to the main layer's thickness. Thus, average velocity in the main layer increases, when operated at constant flow rates, enhancing the convective heat transfer coefficient. This causes the average fluid temperature to approach the lower plate temperature thus reducing the bimaterial effects. When it is operated at a constant pressure or at a constant velocity, the compression of the main layer due to excessive heating at the upper plate reduces the flow rate thus fluid temperatures approach the lower plate temperature at a shorter distance. As such, bimaterial effects are also reduced. It is worth noting that the soft seals can be placed between special guiders as shown in Fig. 1(b). As such, side expansion of the seals can be minimized and the transverse thin film thickness expansion is maximized.

The analysis is concerned with upper and lower thin films that have small thicknesses h_1 and h_2, respectively, compared to their length B and their width D_1 and D_2,

respectively. The x-axis for each layer is taken along the axial direction of the thin film while y-axis for each layer is taken along its thickness as shown in Fig. 1(b). Further, it is assumed that the film thickness is independent of the axial direction. For example, this occurs in symmetric thin films having a fluid injected from the center as shown in Fig. 1(a).

Both lower and upper plates are assumed to be fixed while the intermediate plate is free to move which is separated from the lower and upper plates by flexible complex seals allowing it to move only in the normal direction. The generic motion of the intermediate plate due to both variations of the stagnant fluid temperature in the secondary flow passage and the induced internal pressure pulsations within both main and secondary flow passages is expressed according to the following relation:

$$H_1 = \frac{h_1}{h_0} = (1 + H_T + H_p) \tag{1}$$

where h_0 and H_1 are a reference thickness for the main passage (will be discussed later) and the dimensionless motion of the intermediate plate, respectively. The variables H_T and H_p are the dimensionless motion of the intermediate plate due to both the volumetric thermal expansion of the stagnant fluid and the deformation in seals as a result of the internal pressure forces, respectively. It is assumed that the fluid is Newtonian having constant average properties except for the thermal conductivity.

The general two-dimensional continuity, momentum and energy equations for a laminar thin film are given as

$$\frac{\partial u_i}{\partial x_i} + \frac{\partial v_i}{\partial y_i} = 0 \tag{2}$$

$$\rho_i\left(\frac{\partial u_i}{\partial t} + u_i\frac{\partial u_i}{\partial x_i} + v_i\frac{\partial u_i}{\partial y_i}\right) = -\frac{\partial p_i}{\partial x_i} + \mu_i\left(\frac{\partial^2 u_i}{\partial x_i^2} + \frac{\partial^2 u_i}{\partial y_i^2}\right) \tag{3}$$

$$\rho_i\left(\frac{\partial v_i}{\partial t} + u_i\frac{\partial v_i}{\partial x_i} + v_i\frac{\partial v_i}{\partial y_i}\right) = -\frac{\partial p_i}{\partial y_i} + \mu_i\left(\frac{\partial^2 v_i}{\partial x_i^2} + \frac{\partial^2 v_i}{\partial y_i^2}\right) \tag{4}$$

$$(\rho c_p)_i\left(\frac{\partial T_i}{\partial t} + u_i\frac{\partial T_i}{\partial x_i} + v_i\frac{\partial T_i}{\partial y_i}\right)$$
$$= \frac{\partial}{\partial x_i}\left(k_i\frac{\partial T_i}{\partial x_i}\right) + \frac{\partial}{\partial y_i}\left(k_i\frac{\partial T_i}{\partial y_i}\right) \tag{5}$$

where T, u, v, ρ, p, μ, c_p and k are the fluid temperature, dimensional axial velocity, dimensional normal velocity, average fluid density, pressure, average fluid dynamic viscosity, average specific heat of the fluid and the thermal conductivity of the fluid, respectively. When the fluid contains suspended ultrafine particles, the previous properties will be for the resulting dilute mixture as long

as the diameter of the particles is very small compared to h_0. The index "i" is "1" when analyzing the main layer while it is "2" when analyzing the secondary layer.

Eqs. (2)–(5) are non-dimensionalized using the following dimensionless variables:

$$X_i = \frac{x_i}{B}, \quad Y_i = \frac{y_i}{h_0} \tag{6a, b}$$

$$\tau = \omega t \tag{6c}$$

$$U_i = \frac{u_i}{(\omega B + V_{0i})}, \quad V_i = \frac{v_i}{h_0 \omega} \tag{6d, e}$$

$$\Pi_i = \frac{p_i - p_{ei}}{\mu_i \left(\omega + \frac{V_{0i}}{B}\right)\varepsilon^{-2}} \tag{6f}$$

$$\theta_1 = \frac{T_1 - T_{1o}}{(T_w - T_{1o})}, \quad \theta_2 = \frac{T_2 - T_{2o}}{q_0 h_0 / k_{2o}} \tag{6g, h}$$

where ω, T_{1o}, T_{2o}, T_w, p_e, q_0, k_{2o}, V_{o1} and V_{o2} are the reference frequency of the disturbance, inlet temperature for the main flow, inlet temperature for the secondary flow, lower plate temperature, reference pressure which represents the exit pressure for both layers, reference heat flux at the upper plate, stagnant thermal conductivity of the secondary fluid, reference dimensional velocity for the lower layer and reference dimensional velocity for the upper layer, respectively. The parameter ε appearing in Eq. 6(f) is the perturbation parameter, $\varepsilon = \frac{h_0}{B}$. The prescribed heat at the upper plate, q_u, as well as the dimensionless inlet pressure, Π_{2n}, for the secondary flow vary according to the following generic relationships:

$$q_u = q_0(1 + \beta_q \sin(\gamma \omega t)) \tag{7}$$

$$\Pi_{2n} = \Pi_{2o}(1 + \beta_p \sin(\gamma_p \omega t + \varphi_p)) \tag{8}$$

where β_q, β_p, γ and γ_p are the dimensionless amplitude of upper plate's heat flux, the dimensionless amplitude for the inlet pressure for the secondary flow, dimensionless frequency for the upper plate heat flux and the dimensionless frequency for the inlet pressure for the secondary layer, respectively. The variables X_i, Y_i, τ, U_i, V_i, Π_i and θ_i are the dimensionless forms of x_i, y_i, t, u_i, v_i, p_i and T_i variables, respectively.

For the two-layered thin film shown in Fig. 1(a), the displacement of the intermediate plate due to internal pressure variations is related to the difference in the average dimensionless pressure across the intermediate plate through the theory of the linear elasticity by

$$H_p = E_1^* \frac{(\Pi_{AVG})_1}{\sigma_1} - E_2^* \frac{(\Pi_{AVG})_2}{\sigma_2} \tag{9}$$

where $(\Pi_{AVG})_1$ and $(\Pi_{AVG})_2$ are the average dimensionless pressure in the main and the secondary layers, respectively. The parameter E_i^* will be referred to as the softness index of the supporting seal in layers "1" or "2"

and will be denoted as E^* when $E_1^* = E_2^*$. It has the following functional form:

$$E_i^* = \frac{12 L^* \mu_i \omega D_i}{K^* \varepsilon^3} \tag{10}$$

where K^* is the effective stiffness of the seals that support the intermediate plate. The dimensionless parameter L^* is introduced to account for the elastic contribution of the intermediate plate in the calculation of the displacement.

In this work, the analysis is performed for relatively small thermal load frequencies in order to ascertain that squeezing generated flows are in the laminar regime. For these frequencies, Eq. (9) is applicable and the inertia effect of the intermediate plate is negligible. Moreover, the increase in the thickness due to a pressure increase in the thin film causes a reduction in the stagnant fluid pressure. This action stiffens the sealing assembly. Therefore, the stiffness K^* is considered to be the effective stiffness for the sealing assembly and not for the seal itself. From the practical point of view, the void width G is taken to be large enough such that a small increase in the stagnant fluid pressure due to the thermal expansion can support the associated increase in the elastic force on the seal.

The dimensionless displacement of the intermediate plate due to the thermal expansion is related to the dimensionless average temperature of the upper plate, $(\theta_u)_{AVG}$, by the following linearized model:

$$H_T = -F_T (\theta_u)_{AVG} \tag{11}$$

where F_T is named the dimensionless thermal expansion parameter. It is equal to

$$F_T = A^* \frac{\beta_T q_0 h_0}{k_{2o}} C_F \tag{12}$$

The coefficient A^* depends on the voids dimensions and their geometry. The parameter β_T is the volumetric thermal expansion coefficient of the stagnant fluid in its approximate form: $\beta_T \approx \frac{1}{V_{s0}} \frac{(V_s - V_{s1})}{(T_s - T_{2o})}\big|_{p_{s1}}$ evaluated at the pressure p_{s1} corresponding to the stagnant fluid pressure in the voids when the secondary flow temperature is kept at inlet temperature of the secondary layer T_{2o}. The void volumes V_{s0}, V_{s1} and V_s represent the void volume at the reference condition ($h_2 = h_0$), the void volume when the pressure in the voids is p_{s1} and the void volume at normal operating conditions where the average stagnant fluid temperature is T_s, respectively. The factor C_F represents the volumetric thermal expansion correction factor. This factor is introduced in order to account for the increase in the stagnant pressure due to the increase in the elastic force in the seal during the expansion which tends to decrease the effective volumetric thermal expansion coefficient. It approaches one as the void width G increases and it can be determined theoretically.

The parameter F_T is enhanced at elevated temperatures for liquids and at lower temperatures for gases because β_T increases for liquids and decreases for gases as the temperature increases. Dimensionless thermal expansion parameter is further enhanced by a decrease in k_0, an increase in q_0, an increase in E_i^* or an increase in h_0. It is worth noting that Eq. (11) is based on the assumption that the stagnant fluid temperature is similar to the average upper plate temperature since void surfaces are considered insulated except for the region facing the upper plate in order to provide a maximum volumetric thermal expansion to the voids. Moreover, it is assumed that the heat flux on the upper plate is applied to the portion that faces the secondary flow.

The thermal conductivity of the fluid is considered to vary with the flow speed in order to account for thermal dispersion effects when suspended ultrafine particles are present in the secondary flow. Induced squeezing effects at the intermediate plate due to time variations in the thermal load or inlet pulsative pressures are expected to enhance the heat transfer inside fluid layers due to thermal dispersion effects. To account for this increase, a linear model between the effective thermal conductivity and the fluid speed is utilized [11].

$$k_i(X_i, Y_i, \tau) = (k_0)_i \left(1 + \lambda_i \sqrt{U^2(X_i, Y_i, \tau) + \Lambda_i^2 V^2(X_i, Y_i, \tau)} \right)$$
$$= (k_0)_i \phi_i(X_i, Y_i, \tau) \tag{13}$$

where λ_i and Λ_i are the dimensionless thermal dispersion coefficient and reference squeezing to lateral velocity ratio. They are

$$\lambda_i = C_i^* (\rho c_p)_{fi} h_0 (V_{0i} + \omega B), \quad \Lambda_i = \frac{\varepsilon \sigma_i}{12} \tag{14a, b}$$

The coefficient C^* depends on the diameter of the ultrafine particle, its volume fraction and both fluid and the particle properties. The parameter $(\rho c_p)_{fi}$ is the density times the specific heat of the fluid resulting from the mixture of the pure fluid and the ultrafine particles suspensions within the ith layer while $(k_0)_i$ is the stagnant thermal conductivity of the working fluid in the ith layer that contains ultrafine particles. This stagnant thermal conductivity is usually greater than the thermal conductivity of the pure fluid [12]. It is worth noting that all the fluid properties that appear in Eqs. (2)–(5) need to be replaced by the effective mixture properties which are functions of the pure fluid and the particles and that the diameter of the ultrafine particles are so small that the resulting mixture behaves as a continuum fluid [11].

Flows inside thin films are in laminar regime and could be considered creep flows in certain applications as in lubrication and biological applications. Therefore, the low Reynolds numbers flow model is adopted here. The application of this model to Eqs. (2)–(4) and the results of dimensionalizing the energy equation result in the following reduced non-dimensionalized equations:

$$U_i = \frac{1}{2} \frac{\partial \Pi_i}{\partial X} H_i^2 \left(\frac{Y_i}{H_i} \right) \left(\frac{Y_i}{H_i} - 1 \right) \tag{15}$$

$$V_i = \frac{dH_i}{d\tau} \left(3 \left(\frac{Y_i}{H_i} \right)^2 - 2 \left(\frac{Y_i}{H_i} \right)^3 \right) \tag{16}$$

$$\frac{\partial \Pi_i}{\partial Y_i} = 0 \tag{17}$$

$$\frac{\partial}{\partial X_i} \left(H_i^3 \frac{\partial \Pi_i}{\partial X_i} \right) = \sigma_i \frac{\partial H_i}{\partial \tau} \tag{18}$$

$$(P_S)_i \left(\frac{\partial \theta_i}{\partial \tau} + \frac{12}{\sigma_i} U_i \frac{\partial \theta_i}{\partial X_i} + V_i \frac{\partial \theta_i}{\partial Y_i} \right) = \frac{\partial}{\partial Y_i} \left(\phi_i \frac{\partial \theta_i}{\partial Y_i} \right) \tag{19}$$

The axial diffusion term in the dimensionalized energy equation, Eq. (19), is eliminated because it is of order ε^2. The parameters σ_i and $(P_S)_i$ are called the squeezing number and the thermal squeezing parameter, respectively. They are defined as

$$\sigma_i = \frac{12}{1 + \frac{V_{0i}}{\omega B}}, \quad (P_S)_i = \frac{(\rho c_p)_i h_0^2 \omega}{k_i} \tag{20}$$

The dimensionless thickness of the lower layer and the upper layer are defined as

$$H_1 = \frac{h_1}{h_0}, \quad H_2 = \frac{h_2}{h_0} \tag{21}$$

It is worth noting that the reference thickness h_0 can be determined using the force balance across the intermediate plate due to the flow exit pressures of both layers at static conditions. The reference thickness h_0 can be controlled by either varying flow exit pressures for each layer prior injecting of both flows, by a proper selection to the undistorted thickness of the supporting seals in each layer or by using both methods. Therefore, the dimensionless thicknesses H_1 and H_2 are related to each other through the following relation as both lower and upper plates are fixed:

$$H_1 + H_2 = H_t \tag{22}$$

where H_t is a constant representing the dimensionless total thickness of the two-layered thin film.

Two conditions will be imposed for the inlet flow rate of the main layer. In applications that require minimizations of thermal effects due to an increase in heat transfer from the environment such as for fluidic cells of biological and chemical sensing devices, it is assumed that inlet flow rate for the lower layer is constant. This will be named the CIF condition. However, constant inlet pressure will be assumed to model flow of fluids in combustion applications such as flow of fuel prior to the mixing section. This will be referred as the CIP condition. The previously defined reference velocities V_{o1} and V_{o2} represent the velocity in the flow passages at zero values of the parameters E_1^*, E_2^* and F_T. Accordingly, the

inlet dimensionless pressures are varying with the squeezing numbers according to following relation for the CIP condition:

$$\Pi_{1n} = 12 - \sigma_1 \tag{23}$$

$$\Pi_{2n} = (12 - \sigma_2)(1 + \beta_p \sin(\gamma_p \tau + \varphi_p)) \tag{24}$$

Therefore, the solution of the Reynolds equations for the CIP condition will reveal the following relationships for the dimensionless pressure gradient, the dimensionless pressure and the average dimensionless pressure Π_{AVG} inside lower and upper layers:

$$\frac{\partial \Pi_1(X_1, \tau)}{\partial X_1} = \frac{\sigma_1}{H_1^3} \frac{dH_1}{d\tau} \left(X_1 - \frac{1}{2} \right) - (12 - \sigma_1) \tag{25a}$$

$$\frac{\partial \Pi_2(X_2, \tau)}{\partial X_2} = \frac{\sigma_2}{H_2^3} \frac{dH_2}{d\tau} \left(X_2 - \frac{1}{2} \right) - (12 - \sigma_2)$$
$$\times (1 + \beta_p \sin(\gamma_p \tau + \varphi_p)) \tag{26}$$

$$\Pi_1(X_1, \tau) = \frac{\sigma_1}{2H_1^3} \frac{dH_1}{d\tau} (X_1^2 - X_1) - (12 - \sigma_1)(X_1 - 1) \tag{27a}$$

$$\Pi_2(X_2, \tau) = \frac{\sigma_2}{2H_2^3} \frac{dH_2}{d\tau} (X_2^2 - X_2) - (12 - \sigma_2)(X_2 - 1)$$
$$\times (1 + \beta_p \sin(\gamma_p \tau + \varphi_p)) \tag{28}$$

$$(\Pi_{AVG}(\tau))_1 = -\frac{\sigma_1}{12H_1^3} \frac{dH_1}{d\tau} + \frac{(12 - \sigma_1)}{2} \tag{29a}$$

$$(\Pi_{AVG}(\tau))_2 = -\frac{\sigma_2}{12H_2^3} \frac{dH_2}{d\tau} + \frac{(12 - \sigma_2)}{2}$$
$$\times (1 + \beta_p \sin(\gamma_p \tau + \varphi_p)) \tag{30}$$

For the CIF condition, the dimensionless pressure gradient, the dimensionless pressure and the average dimensionless pressure Π_{AVG} inside lower layer will be changed to the following:

$$\frac{\partial \Pi_1(X_1, \tau)}{\partial X_1} = \frac{\sigma_1}{H_1^3} \frac{dH_1}{d\tau} X_1 - \frac{(12 - \sigma_1)}{H_1^3} \tag{25b}$$

$$\Pi_1(X_1, \tau) = \frac{\sigma_1}{2H_1^3} \frac{dH_1}{d\tau} (X_1^2 - 1) - \frac{(12 - \sigma_1)}{H_1^3} (X_1 - 1) \tag{27b}$$

$$(\Pi_{AVG}(\tau))_1 = -\frac{\sigma_1}{3H_1^3} \frac{dH_1}{d\tau} + \frac{(12 - \sigma_1)}{2H_1^3} \tag{29b}$$

2.1. Thermal boundary conditions

The dimensionless initial and thermal boundary conditions for the previously defined problem are taken as follows:

$$\theta_1(X_1, Y_1, 0) = 0, \quad \theta_1(0, Y_1, \tau) = 0,$$
$$\theta_1(X_1, 0, \tau) = 1, \quad \frac{\partial \theta_1(X_1, H_1, \tau)}{\partial Y_1} = 0, \tag{31}$$

$$\theta_2(X_2, Y_2, 0) = 0, \quad \theta_2(0, Y_2, \tau) = 0,$$
$$\frac{\partial \theta_2(X_2, 0, \tau)}{\partial Y_2} = -(1 + \beta_q \sin(\gamma \tau)),$$
$$\frac{\partial \theta_2(X_2, H_2, \tau)}{\partial Y_2} = 0 \tag{32}$$

Based on physical conditions, the intermediate plate is taken to be insulated and the Nusselt number at the lower and the upper plates are defined as

$$Nu_l(X_1, \tau) \equiv \frac{h_{cl} h_0}{k_1} = -\frac{1}{1 - \theta_{1m}} \frac{\partial \theta_1(X_1, 0, \tau)}{\partial Y_1} \tag{33}$$

$$Nu_u(X_2, \tau) \equiv \frac{h_{cu} h_0}{k_2} = \frac{1}{\theta_2(X_2, 0, \tau) - \theta_{2m}(X_2, \tau)}$$
$$= \frac{1}{\theta_u(X_2, \tau) - \theta_{2m}(X_2, \tau)} \tag{34}$$

where h_{cl} and h_{cu} are the convective heat transfer coefficients for the lower and upper plates, respectively. The quantities θ_{im} and U_{im} are the sectional dimensionless mean bulk temperature and the dimensionless average velocity for the ith layer. They are given as

$$\theta_{im}(X_i, \tau) = \frac{1}{U_{im}(X_i, \tau) H_i} \int_0^{H_i} U_i(X_i, Y_i, \tau) \theta_i(X_i, Y_i, \tau) \, dY_i$$
$$U_{im}(X_i, \tau) = \frac{1}{H_i} \int_0^{H_i} U_i(X_i, Y_i, \tau) \, dY_i \tag{35}$$

where U_{im} is the dimensionless average velocity at a given section for the ith layer. For the main passage, the dimensionless heat flux at a given section is defined as follows

$$\Theta(X_1, \tau) = -\frac{\partial \theta_1(X_1, 0, \tau)}{\partial Y_1} \tag{36}$$

2.2. Dimensionless flow rate parameter for the main layer

It is worth noting that the obtained dimensionless film thickness for the main layer H_1 can be used to determine the dimensionless flow rate of the fluid in the main passage at the mid section for the CIP condition. The latter is an important parameter that needs to be controlled. This term is referred to as $\Psi_{X=0.5}$ where $X = 0.5$ denotes the location at $X_1 = 0.5$. It can be calculated from the following relation

$$\Psi_{X=0.5} = \frac{Q_{X=0.5}}{(V_{o1} + \omega B) h_0} = \frac{(12 - \sigma_1)}{12} H_1^3 \tag{37}$$

where $Q_{X=0.5}$ is the dimensional flow rate at $X = 0.5$ in the main thin film.

3. Numerical procedure

The procedure for the numerical solution is summarized as follows:

1. Initially, a value for H_T is assumed.
2. The dimensionless thicknesses for the lower and upper layers H_1 and H_2 are determined by solving Eqs. (1), (9), (22), (29) and (30), simultaneously, using an explicit formulation. The velocity field, U_i and V_i, is then determined from Eqs. (15), (16), (25) and (26).
3. Reduced energy equations, Eq. (19), are solved by first transferring them to a constant boundary domain using the following transformations: $\tau^* = \tau$, $\xi_i = X_i$ and $\eta_i = \frac{Y_i}{H_i}$. Tri-diagonal algorithm (Blottner [13]) was implemented along with a marching scheme. Backward differencing was chosen for the axial convective and transient terms and central differencing was selected for the derivatives with respect to η_i. The values of 0.008, 0.03, 0.001 were chosen for $\Delta\xi_i, \Delta\eta_i$ and $\Delta\tau^*$, respectively.
4. H_T is updated from Eq. (11) and steps (2)–(4) is repeated until

$$\left| \frac{(H_T)_{\text{new}} - (H_T)_{\text{old}}}{(H_T)_{\text{new}}} \right| < 10^{-6} \tag{38}$$

5. The solution for the flow and heat transfer inside the two layers is determined.
6. Time is advanced by $\Delta\tau^*$ and steps (1)–(5) are repeated.

Numerical investigations were performed using different mesh sizes and time steps to assess and ascertain grid and time step independent results. It was found that any reduction in the values of $\Delta\xi, \Delta\eta$ and τ^* below $\Delta\xi = 0.008$, $\Delta\eta = 0.03$ and $\Delta\tau^* = 0.001$ cause less than 0.2% error in the results.

The maximum value of the parameters P_S is chosen to be 1.0. Beyond this value, the error associated with the low Reynolds number model will increase for moderate values of the dimensionless thermal expansion parameter, softness index of the seals, and the Prandtl number. As an example, the order of transient and convective terms in the momentum equations is expected to be less than 5.0% that of the diffusive terms for $P_S = 1.0$, $Pr = 6.7$, $E_1^* = E_2^* = 0.3$, $F_T = 0.15$, $\beta_q = 0.2$ and $\sigma_1 = 3.0$, $\sigma_2 = 6.0$. The parameters correspond, for example, to a main thin film filled with water and having $B = D = 60$ mm, $h_0 = 0.3$ mm, $\omega = 1.7$ s^{-1}, $V_0 = 0.1$ m/s and $K^* = 33\,000$ N/m.

4. Discussions of the results

Ideal gases produce approximately a 15% increase in the void volume under typical room conditions for a 45 °C temperature difference. Further, Li and Xuan [14] reported a 60% increase in the convective heat transfer coefficient for a 2% volume fraction of copper ultrafine particles. Accordingly, the parameters F_T and λ_2 were varied until comparable changes have been attained in the dimensionless thin film thickness and the Nusselt number.
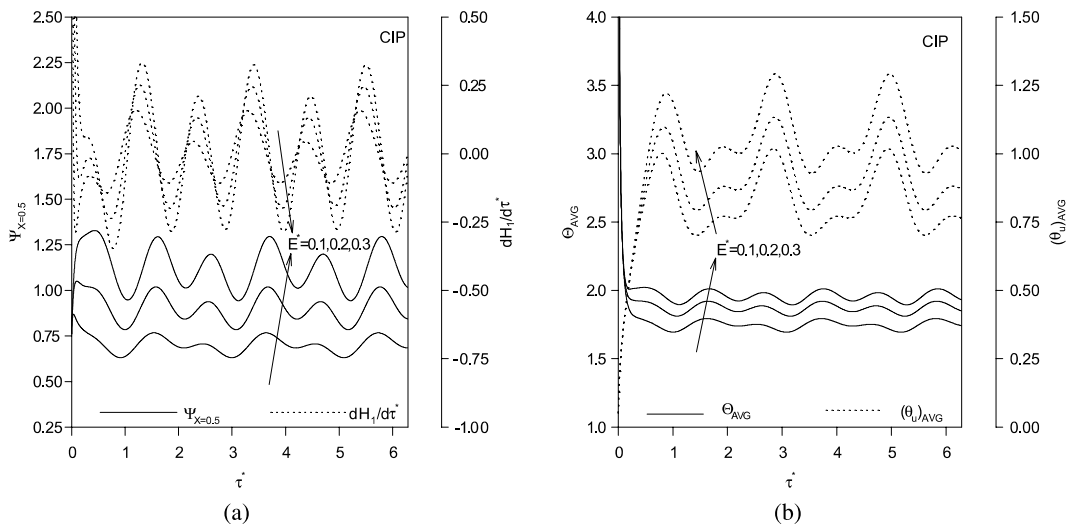
Fig. 2. Effects of E^* on (a) $\Psi_{X=0.5}$ and $dH_1/d\tau^*$, (b) Θ_{AVG} and $(\theta_u)_{\text{AVG}}$ ($H_t = 2.0$, $F_T = 0.15$, $P_{S1} = P_{S2} = 1.0$, $\beta_p = 0.3$, $\beta_q = 0.2$, $\varphi_p = \pi/2$, $\gamma = 3.0$, $\gamma_p = 6.0$, $\lambda_1 = \lambda_2 = 0$, $\sigma_1 = 3.0$, $\sigma_2 = 6.0$).

4.1. The role of the softness index and the thermal expansion parameters of the seal

Fig. 2 illustrates the effects of the softness index of the supporting seals on the dynamics and thermal characterizations of a two-layered thin film operating at CIP condition. The softness index is considered to be equal for both layers, denoted by E^*. This corresponds to the case when both lower and upper layers fluids are identical. As the softness index E^* increases, the dimensionless flow rate parameter for the main layer $\Psi_{X=0.5}$ increases as described by the solid lines displayed in Fig. 2(a). This is expected for cases where the average pressure of the lower layer is greater than that of the upper layer. Meanwhile the disturbance in the main layer thickness increases as E^* increases as depicted by the dotted line shown in Fig. 2(b). This phenomenon can be utilized in enhancing the cooling due to thermal dispersion in the secondary flow as proposed by Eq. (13). On the other hand, these disturbances may cause malfunctioning of any sensing devices placed in the flow passage since both flow dynamical effects and chemical reactions will be affected. The increase in $\Psi_{X=0.5}$ as E^* increases causes an increase in the average dimensionless heat transfer Θ_{AVG} in the main layer and an increase in the average upper plate temperature $(\theta_u)_{AVG}$ as shown in Fig. 2(b) due to the shrinkage in the upper layer.

For the CIP condition, the increase in the dimensionless thermal expansion parameter F_T of the upper flexible complex seals causes a reduction in $\Psi_{X=0.5}$ values and an increase in the disturbance at intermediate plate. Consequently, the parameters Θ_{AVG} and $(\theta_u)_{AVG}$ decrease as F_T increases. These observations are shown in Fig. 3 which corresponds to a parametric case with

water as the main fluid while the secondary fluid is taken to be air. For CIF condition, the compression in the main layer film thickness increases the flow near the lower and intermediate plates thus enhancing the thermal convection as illustrated in Fig. 4. As a result, thermally developed conditions are achieved within shorter distance from the inlet as F_T increases. This alleviates thermal effects such as bimaterial effects in sensors.
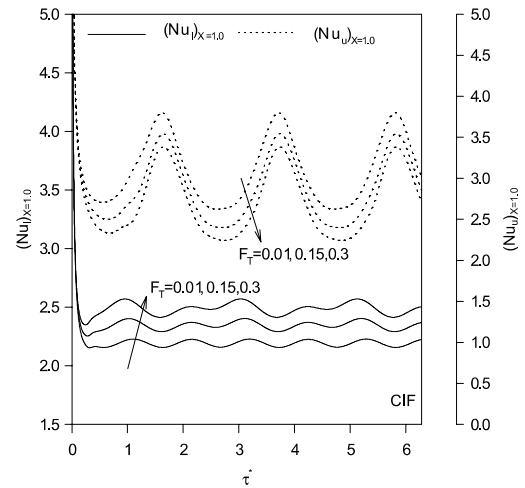
Fig. 4. Effects of F_T on Nusselt numbers for main and secondary flows: (main flow maintained at a CIF condition, $H_t = 2.0$, $E^* = 0.2$, $P_{S1} = P_{S2} = 1.0$, $\beta_p = 0.3$, $\beta_q = 0.2$, $\varphi_p = \pi/2$, $\gamma = 3.0$, $\gamma_p = 6.0$, $\lambda_1 = \lambda_2 = 0$, $\sigma_1 = 3.0$, $\sigma_2 = 6.0$).
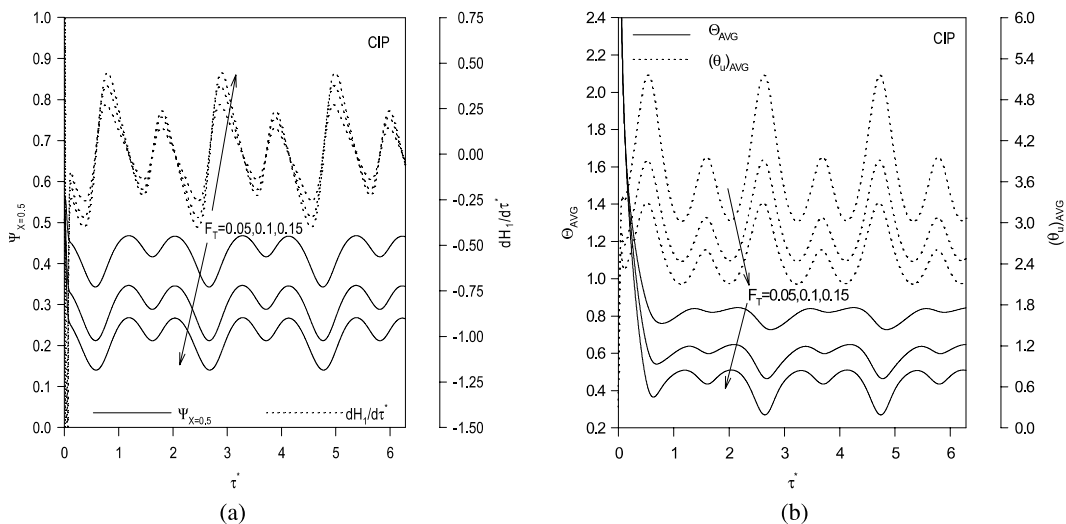
Fig. 3. Effects of F_T on (a) $\Psi_{X=0.5}$ and $dH_1/d\tau^*$, (b) Θ_{AVG} and $(\theta_u)_{AVG}$ ($H_t = 2.0$, $E_1^* = 0.3$, $E_2^* = 0.003$, $P_{S1} = 1.0$, $P_{S2} = 0.012$, $\beta_p = 0.3$, $\beta_q = 0.2$, $\varphi_p = \pi/2$, $\gamma = 3.0$, $\gamma_p = 6.0$, $\lambda_1 = \lambda_2 = 0$, $\sigma_1 = 6.0$, $\sigma_2 = 1.0$).

4.2. The role of the squeezing and thermal squeezing parameters

As the squeezing number for the main flow passage increases, the net pressure force on the intermediate plate decreases as dictated by Eq. (9). Therefore, the main layer film thickness decreases causing a reduction in the values of $\Psi_{X=0.5}$, Θ_{AVG} and $(\theta_u)_{\text{AVG}}$ as shown in Fig. 5. It is noticed that the disturbance at the intermediate plate, variation in $dH_1/d\tau$, decreases slightly as σ_1 increases as shown in Fig. 5(a). This phenomenon is ascribed to the fact that the relief in the thickness of the upper layer tend to minimize the effects of the internal pressure pulsations on the moving plate. This phenomenon can also be recognized in Fig. 2(a).

The increase in the value of the thermal squeezing parameter P_{S2} of the upper layer causes an enhancement in the upper plate cooling as shown by reductions in $(\theta_u)_{\text{AVG}}$ in Fig. 6(b). By introducing salt concentrations or due to the presence of scales in the secondary fluid, the value of P_{S2} can be altered. This will cause an increase in E_2^* which can be kept constant by a proper choice of the upper layer width D_2. Due to reductions in $(\theta_u)_{\text{AVG}}$ as P_{S2} increases, the upper layer film thickness
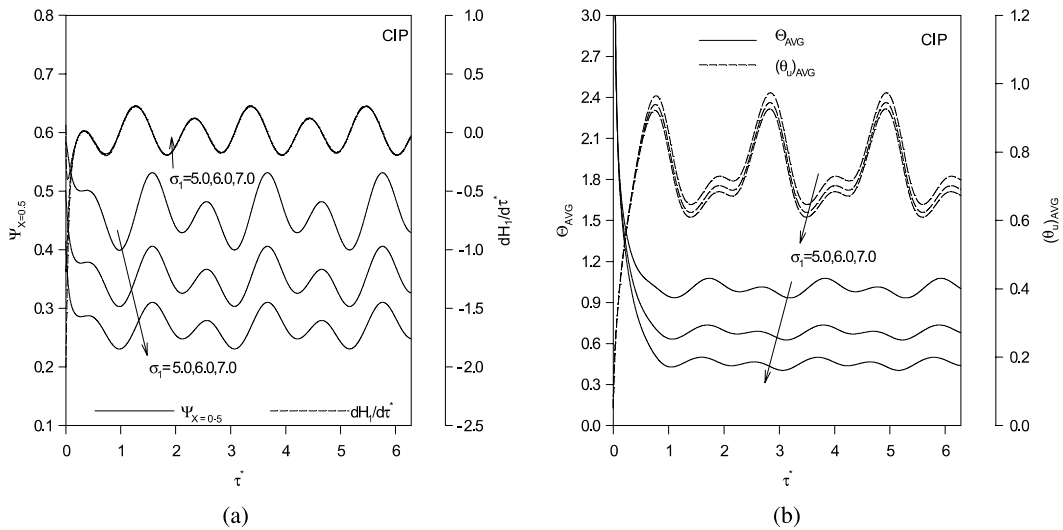
Fig. 5. Effects of σ_1 on (a) $\Psi_{X=0.5}$ and $dH_1/d\tau^*$, (b) Θ_{AVG} and $(\theta_u)_{\text{AVG}}$ ($H_t = 2.0$, $E^* = 0.2$, $F_T = 0.15$, $P_{S1} = P_{S2} = 1.0$, $\beta_p = 0.3$, $\beta_q = 0.2$, $\varphi_p = \pi/2$, $\gamma = 3.0$, $\gamma_p = 6.0$, $\lambda_1 = \lambda_2 = 0$, $\sigma_2 = 6.0$).
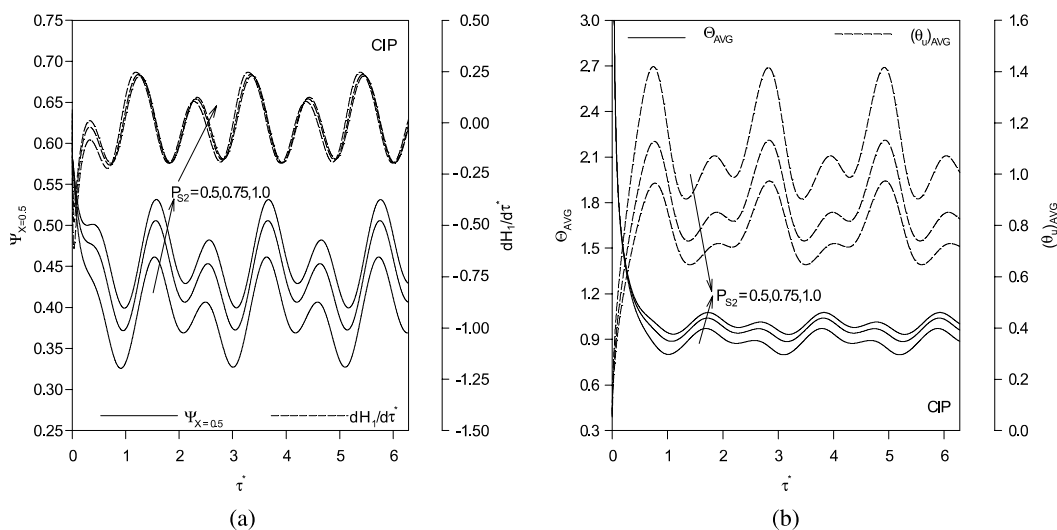
Fig. 6. Effects of P_{S2} on (a) $\Psi_{X=0.5}$ and $dH_1/d\tau^*$, (b) Θ_{AVG} and $(\theta_u)_{\text{AVG}}$ ($H_t = 2.0$, $E^* = 0.2$, $F_T = 0.15$, $P_{S1} = 1.0$, $\beta_p = 0.3$, $\beta_q = 0.2$, $\varphi_p = \pi/2$, $\gamma = 3.0$, $\gamma_p = 6.0$, $\lambda_1 = \lambda_2 = 0$, $\sigma_1 = 5.0$, $\sigma_2 = 6.0$).
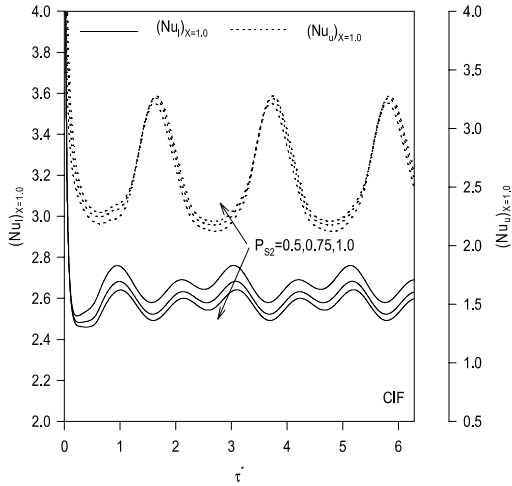
Fig. 7. Effects of P_{S2} on Nusselt numbers for main and secondary flows: (main flow maintained at a CIF condition, $H_t = 2.0$, $E^* = 0.2$, $F_T = 0.15$, $P_{S1} = 1.0$, $\beta_p = 0.3$, $\beta_q = 0.2$, $\varphi_p = \pi/2$, $\gamma = 3.0$, $\gamma_p = 6.0$, $\lambda_1 = \lambda_2 = 0$, $\sigma_1 = 5.0$, $\sigma_2 = 6.0$).

decreases allowing for more flooding in the main layer. Thus, the average heat transfer in the main layer increases as P_{S2} increases (Fig. 6). The variation in $dH_1/d\tau$ decreases slightly as P_{S2} increases due to reductions in H_T noting that the intermediate plate becomes more stable for the effects that makes it closer to either the upper or lower plates for a given softness index. The increase in the cooling of the upper layer due to an increase in P_{S2} causes a relief in the main layer film thickness resulting in a reduction in its Nusselt number (Fig. 7 for the CIF condition). Accordingly, the main inlet temperature is

convected further downstream which may increase noise levels due bimaterial effects of certain sensors.

4.3. The role of thermal dispersion due to ultrafine suspensions

Due to their random motions, ultrafine particles tend to increase the heat exchange within the fluid causing the thermal dispersion effect. Therefore, as the dimensionless thermal dispersion parameter λ increases, the thermal conductivity increases causing the upper plate temperature $(\theta_u)_{AVG}$ to decrease. Thus in turn, the values of $\Psi_{X=0.5}$ and Θ_{AVG} are increased while variations in $dH_1/d\tau$ are decreased as λ increases (Fig. 8 for the CIP condition). As such, the stability of the intermediate plate is enhanced in the presence of dispersive flows. In case of the CIF condition, the relief in the main layer film thickness due to an increase in λ as shown in Fig. 9(a) reduces the convective heat transfer coefficient of the main layer. Thus, a decrease in Θ_{AVG} is associated as shown in Fig. 9(b).

4.4. The role of the pulsation frequency and the total thickness of the two layers

Fig. 10 shows the effects the frequency of pressure pulsation γ_p on fluctuations of $\Psi_{X=0.5}$ and $(\theta_u)_{AVG}$. These fluctuations are defined as

$$\Delta\Psi_{X=0.5} = \frac{(\Psi_{X=0.5})_{max} - (\Psi_{X=0.5})_{min}}{2},$$
$$\Delta\Theta_{AVG} = \frac{(\Theta_{AVG})_{max} - (\Theta_{AVG})_{min}}{2} \tag{39}$$
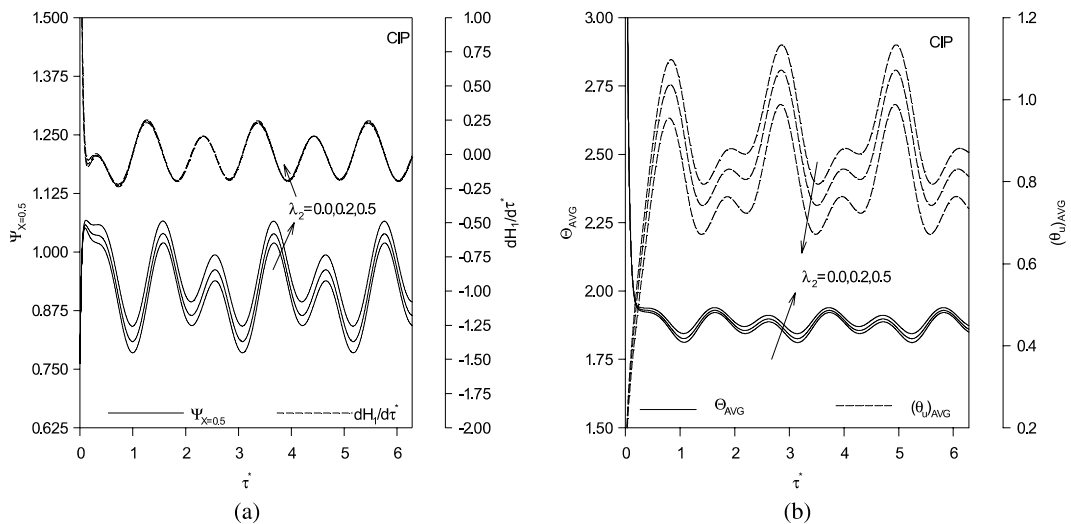
(a)   (b)

Fig. 8. Effects of λ_2 on (a) $\Psi_{X=0.5}$ and $dH_1/d\tau^*$, (b) Θ_{AVG} and $(\theta_u)_{AVG}$ (main flow maintained at a CIP condition, $H_t = 2.0$, $E^* = 0.2$, $F_T = 0.15$, $P_{S1} = P_{S2} = 1.0$, $\beta_p = 0.3$, $\beta_q = 0.2$, $\varphi_p = \pi/2$, $\gamma = 3.0$, $\gamma_p = 6.0$, $\lambda_1 = 0$, $\sigma_1 = 3.0$, $\sigma_2 = 6.0$).
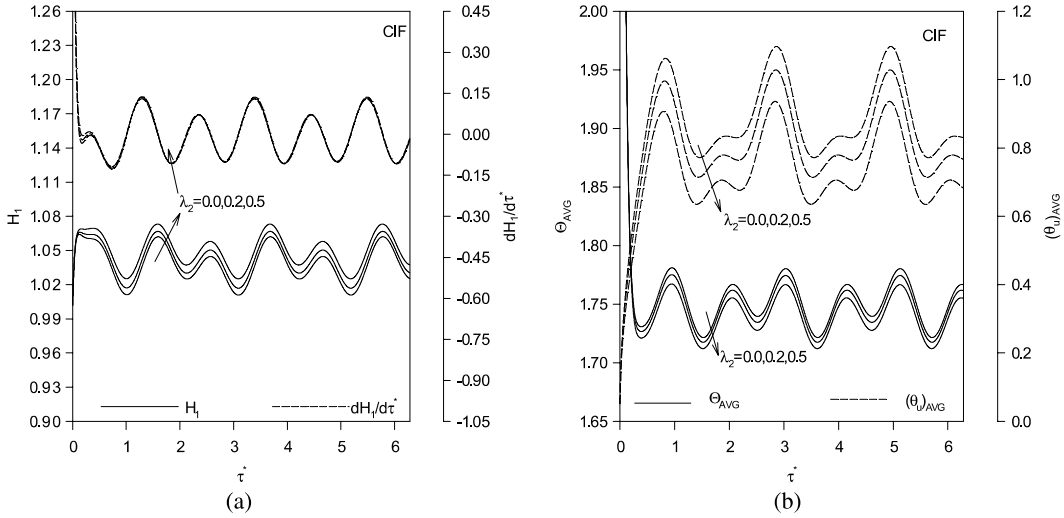
Fig. 9. Effects of λ_2 on (a) $\Psi_{X=0.5}$ and $dH_1/d\tau^*$, (b) Θ_{AVG} and $(\theta_u)_{AVG}$ (main flow maintained at a CIF condition, $H_t = 2.0$, $E^* = 0.2$, $F_T = 0.15$, $P_{S1} = P_{S2} = 1.0$, $\beta_p = 0.3$, $\beta_q = 0.2$, $\varphi_p = \pi/2$, $\gamma = 3.0$, $\gamma_p = 6.0$, $\lambda_1 = 0$, $\sigma_1 = 3.0$, $\sigma_2 = 6.0$).
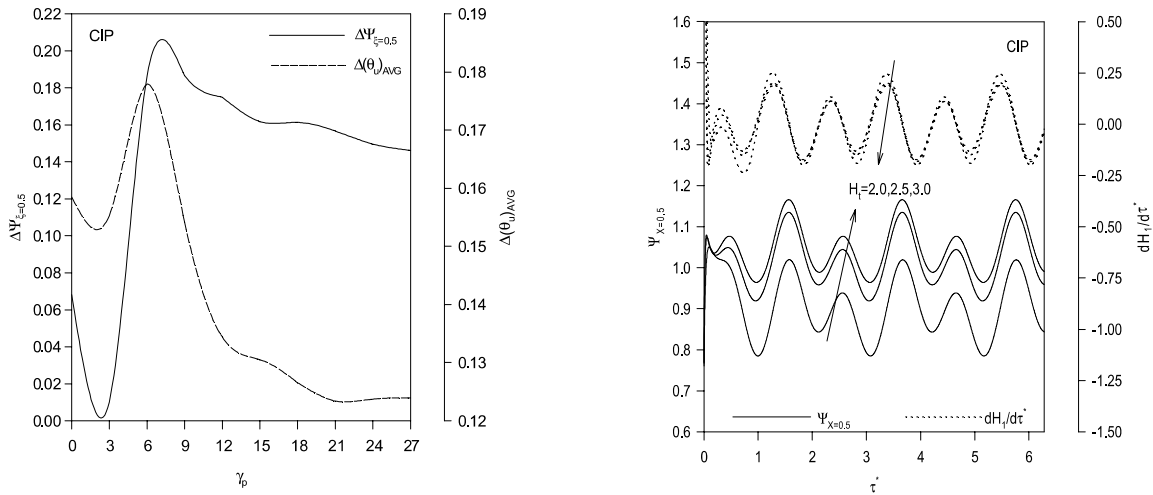
Fig. 10. Effects of γ_p on $\Delta\Psi_{X=0.5}$ and $\Delta(\theta_u)_{AVG}$ for the CIP condition ($H_t = 2.0$, $E^* = 0.3$, $F_T = 0.3$, $P_{S1} = P_{S2} = 1.0$, $\beta_p = 0.3$, $\beta_q = 0.2$, $\varphi_p = \pi/2$, $\gamma = 3.0$, $\lambda_1 = \lambda_2 = 0$, $\sigma_1 = 3.0$, $\sigma_2 = 6.0$).

Fig. 11. Effects of H_t on $\Psi_{X=0.5}$ and $dH_1/d\tau^*$ (main flow maintained at a CIP condition, $E^* = 0.2$, $F_T = 0.15$, $P_{S1} = P_{S2} = 1.0$, $\beta_p = 0.3$, $\beta_q = 0.2$, $\varphi_p = \pi/2$, $\gamma = 3.0$, $\gamma_p = 6.0$, $\lambda_1 = \lambda_2 = 0$, $\sigma_1 = 3.0$, $\sigma_2 = 6.0$).

where the maximum and minimum values corresponds to the steady periodic values. It should be noted that $\Delta\Psi_{X=0.5}$ and $\Delta\Theta_{AVG}$ are unpredictable at relatively lower frequencies of pulsations and the main layer becomes more stable for large values of γ_p (Fig. 10). Finally, Fig. 11 shows that the reduction in the main layer flow rate decreases as the dimensionless total thickness H_t increases. This is because more cooling is expected to the upper plate as H_t increases resulting in reducing the volumetric thermal expansion effects of the stagnant fluid. As such, the fluctuating rate at the intermediate

plate is reduced as H_t increases for the selected range as shown in Fig. 11.

5. Conclusions

Flow and heat transfer within a two-layered thin film channel supported by flexible complex seals have been analyzed in this work in the presence of suspended ultrafine particles. Thermal load and the inlet pressure pulsations of the secondary layer were generically prescribed. The governing continuity, momentum equa-

tions and energy equations for both layers were non-dimensionalized and categorized based low Reynolds numbers flow model. The deformation of the supporting seals was related to the internal pressure difference and the upper plate temperature through the theory of linear elasticity and the volumetric thermal expansion effects of the flexible complex seal. The velocity field and the solution of the energy equation were found using an iterative scheme and a marching technique in both the axial direction and the time domain.

It was found that the flow rate and the average heat transfer in the main thin film channel can be increased by an increase in the softness index of the seals, the thermal squeezing parameter and the thermal dispersion effect while they are decreased as the thermal expansion parameter of the complex seal and the squeezing number of the main layer increase. The increase in thermal dispersion and the increase in the thermal squeezing parameter of the secondary layer were found to increase the stability of the moving plate separating the two layers. For constant flow conditions, the main layer Nusselt number was found to increase by an increase in the thermal expansion parameter, and a decrease in both the thermal dispersion and the thermal squeezing parameters of the secondary layer. The proposed two-layered thin film channel is found to be more stable at large pulsation frequencies. Finally, the two-layered thin film was found to provide a self-regulating tool for the flow rate and temperature of the main fluid chamber under extreme conditions.

Acknowledgements

References

[1] A.G. Fedorov, R. Viskanta, Three-dimensional conjugate heat transfer in the microchannel heat sink for electronic packaging, Int. J. Heat Mass Transfer 43 (2000) 399–415.

[2] K. Vafai, L. Zhu, Analysis of a two-layered micro channel heat sink concept in electronic cooling, Int. J. Heat Mass Transfer 42 (1999) 2287–2297.

[3] A.Z. Sezri, Tribology, Hemisphere, New York, 1980, 10–12.

[4] N.V. Lavrik, C.A. Tipple, M.J. Sepaniak, D. Datskos, Gold nano-structure for transduction of biomolecular interactions into micrometer scale movements, Biomed. Microdev. 31 (2001) 35–44.

[5] J. Fritz, M.K. Baller, H.P. Lang, H. Rothuizen, P. Vettiger, E. Meyer, H.-J. Güntherodt, Ch. Gerber, J.K. Gimzewski, Translating biomolecular recognition into nanomechanics, Science 288 (2000) 316–318.

[6] W.E. Langlois, Isothermal squeeze films, Quart. Appl. Math. XX (1962) 131–150.

[7] A.R.A. Khaled, K. Vafai, Nonisothermal characterization of thin film oscillating bearings, Numer. Heat Transfer Part A 41 (2002) 451–467.

[8] A.-R.A. Khaled, K. Vafai, Analysis of flow and heat transfer inside oscillatory squeezed thin films subject to a varying clearance, Int. J. Heat Mass Transfer 46 (2003) 631–641.

[9] A.R.A. Khaled, K. Vafai, Flow and heat transfer inside thin films supported by soft seals in the presence of internal and external pressure pulsations, Int. J. Heat Mass Transfer 45 (2002) 5107–5115.

[10] A.R.A. Khaled, K. Vafai, Cooling enhancements in thin films supported by flexible complex seals in the presence of ultrafine suspensions, ASME J. Heat Transfer 125 (2003) 916–925.

[11] Y. Xuan, W. Roetzel, Conceptions for heat transfer correlation of nanofluids, Int. J. Heat Mass Transfer 43 (2000) 3701–3707.

[12] J.A. Eastman, S.U.S. Choi, S. Li, W. Yu, L.J. Thompson, Anomalously increased effective thermal conductivities of ethylene glycol-based nanofluids containing copper nanoparticles, Appl. Phys. Lett. 78 (2001) 718–720.

[13] F.G. Blottner, Finite-difference methods of solution of the boundary-layer equations, AIAA Journal 8 (1970) 193–205.

[14] Q. Li, Y. Xuan, Convective heat transfer and flow characteristics of Cu–water nanofluid, Sci. China (Series E) 45 (2002) 408–416.